Integrated Remote Sensing in the Exploration of the Amacan Geothermal Prospect Davao de Oro, Philippines

By

Jeffrey Bermido, Kevin Paul Guillermo, Oliver Briola, Leonardo Morales, Releo Contemplacion, and Joeffrey Caranto

Energy Development Corporation

Presented By

Jeffrey Bermido

Energy Development Corporation

14th NCS National Convention on Statistics
1-3 October 2019 | Crowne Plaza Manila Galleria
Organized by the Philippine Statistical System
Spearheaded by the Philippine Statistics Authority

GEOTHERMAL ENERGY
Geo = Earth;Thermal = Heat

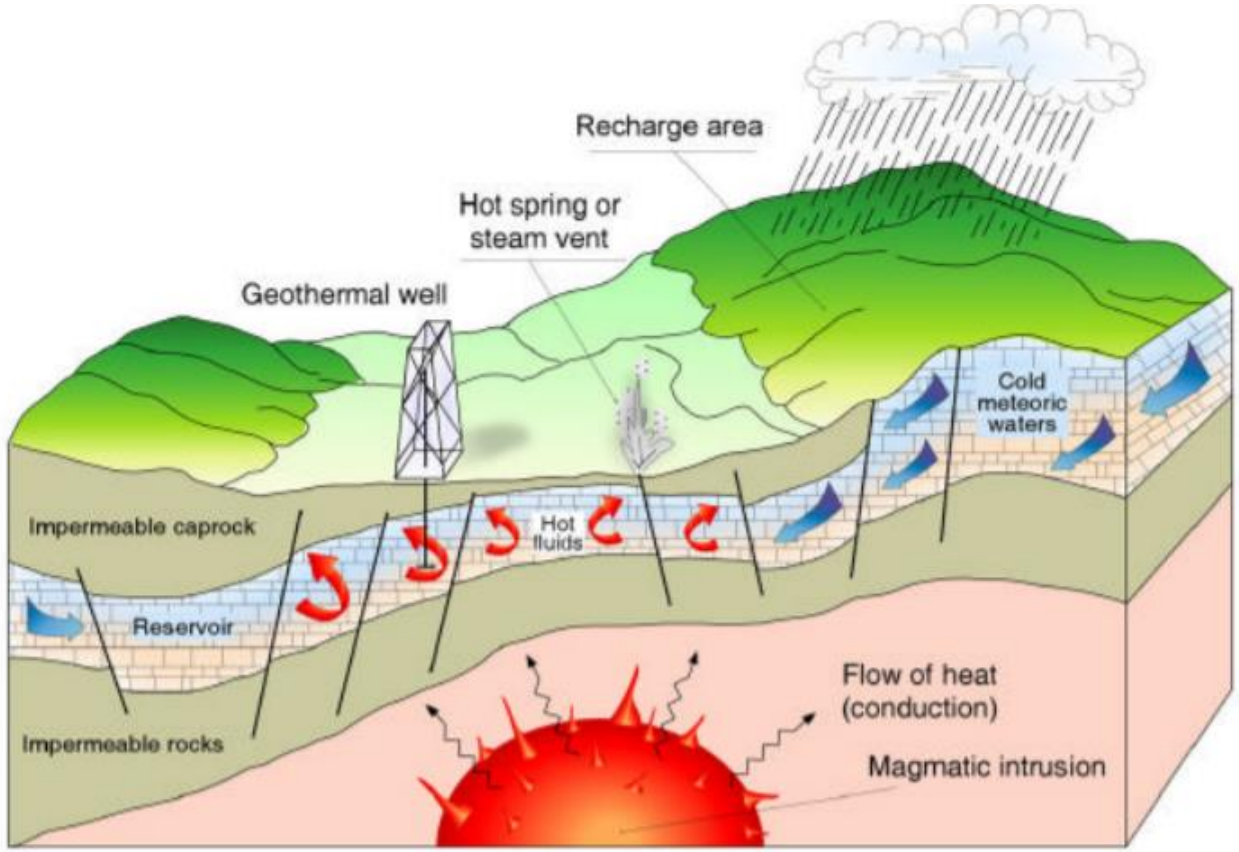

http://users.metu.edu.tr/mahmut/pete450/Dickson.pdf

In exploration, we look for

Thermal manifestations

Geologic structures

Hydrothermal Alteration

AMACAN GEOTHERMAL PROSPECT

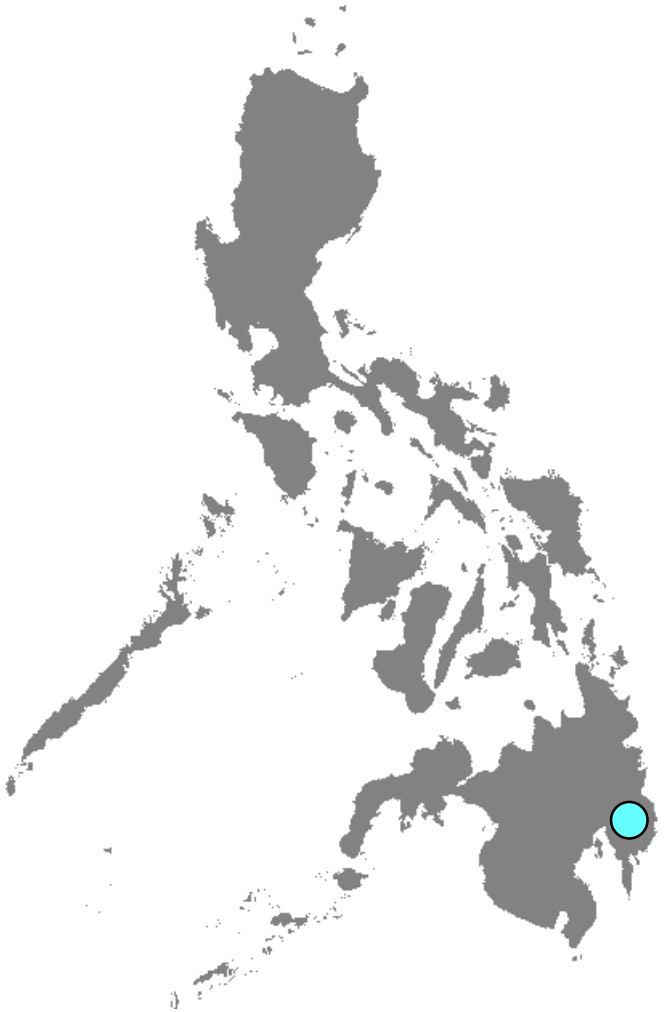

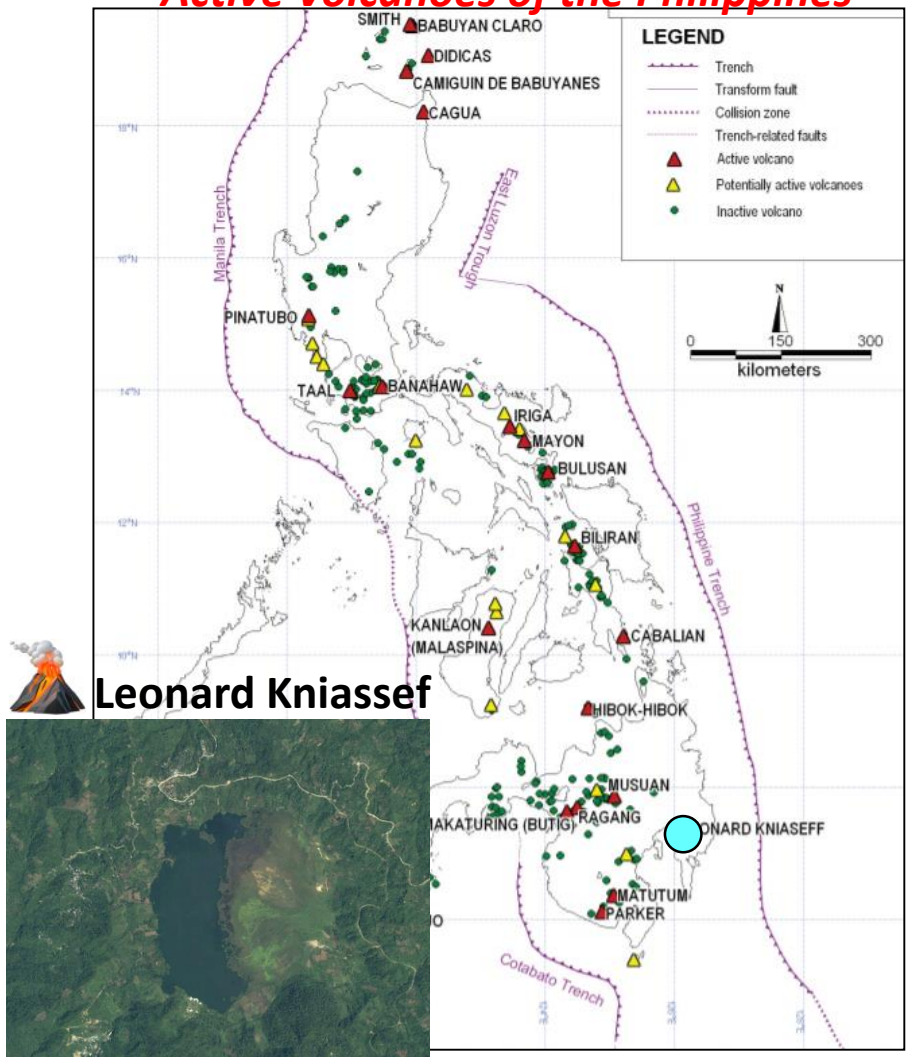

Leonard Kniassef

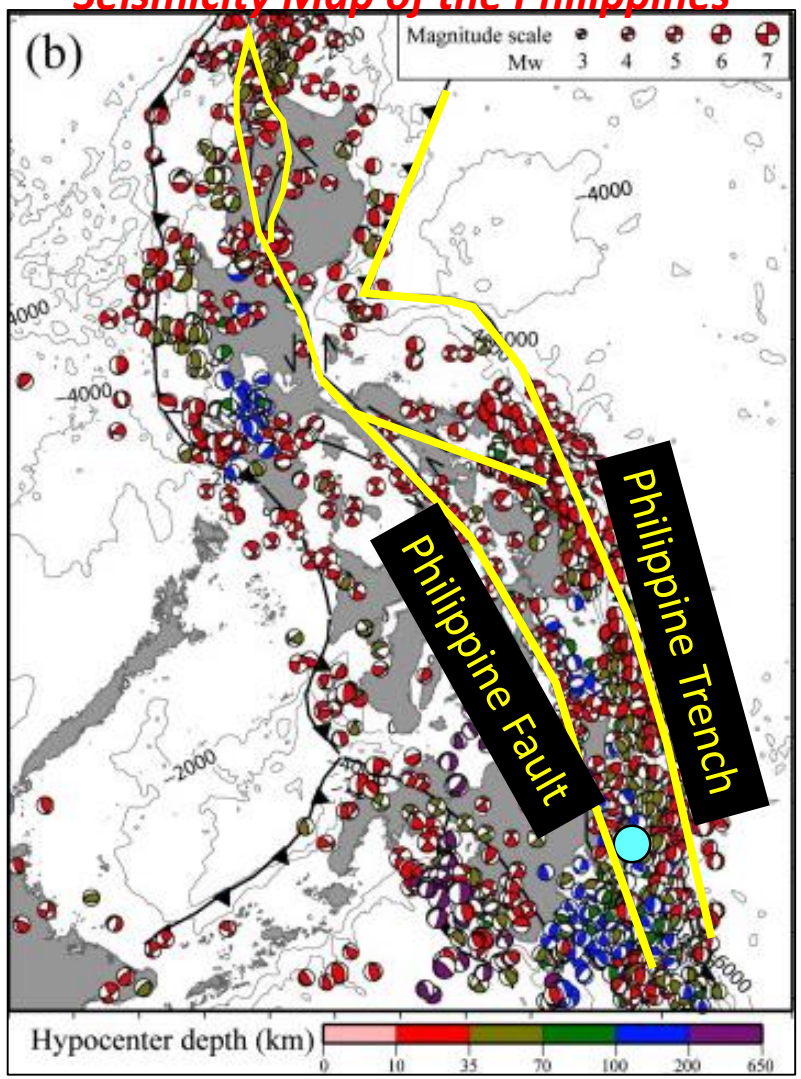

PHIVOLCS

MATERIALS AND METHODS

REMOTE SENSING

DEM → **SLOPE AND LINEAMENT ANALYSIS**

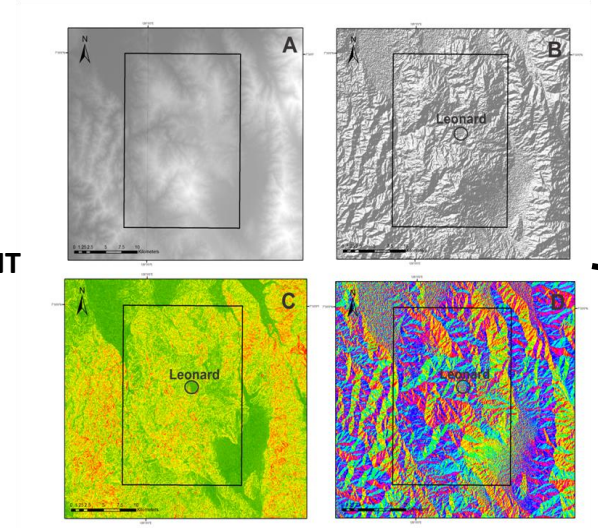

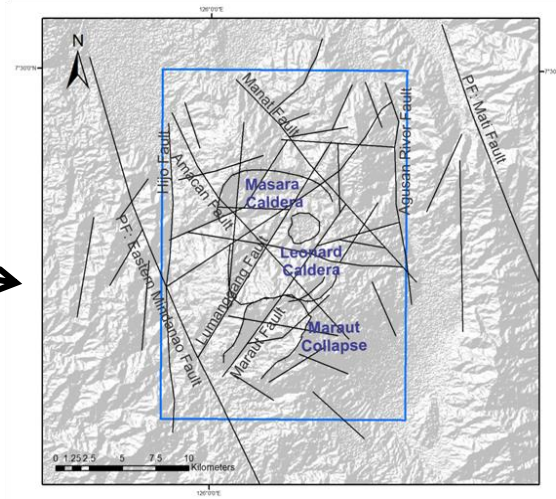

Lineament Map

LANDSAT 8 →

HYDROTHERMAL ALTERATION

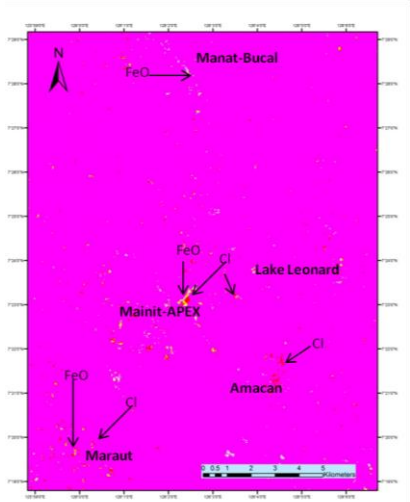

THERMAL MAPPING

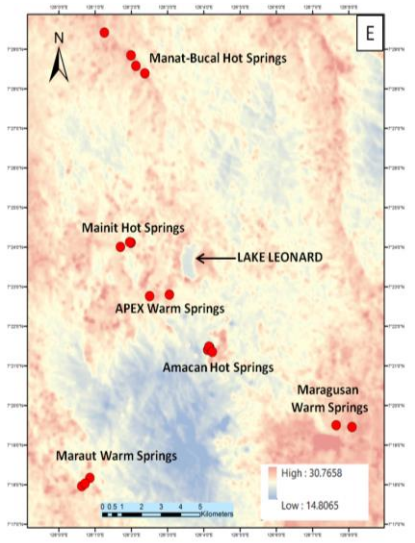

SLOPE ASPECT STATISTICS

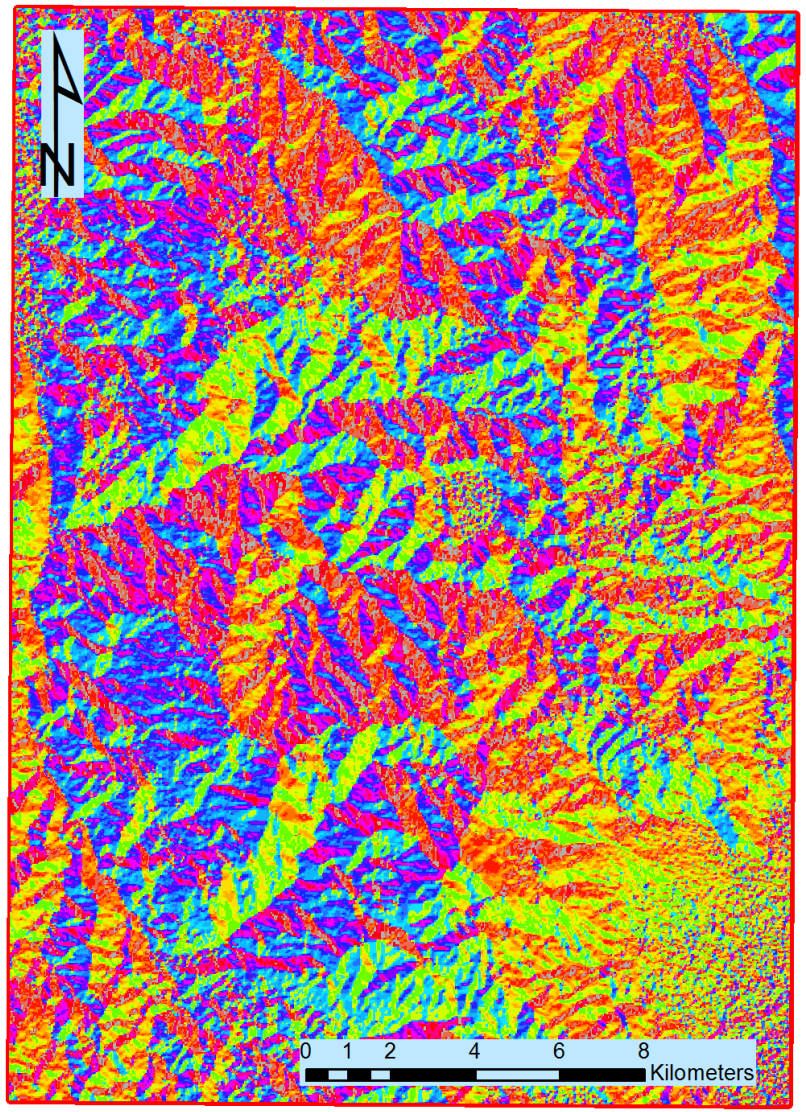

Legend

- -1 - 017° (Flat to NNE)
- 017° - 037° (NE)
- 037° - 057° (NE)
- 057° - 077° (NE)
- 077° - 097° (ENE to ESE)
- 097° - 118° (ESE)
- 118° - 138° (SE)
- 138° - 157° (SE)
- 157° - 177° (SSE)
- 177° - 198° (SSE to SSW)
- 198° - 218° (SW)
- 218° - 240° (SW)
- 240° - 259° (SW)
- 259° - 279° (WSW to WNW)
- 279° - 299° (NW)
- 299° - 318° (NW)
- 319° - 339° (NW)
- 339° - 360° (NNW to N)

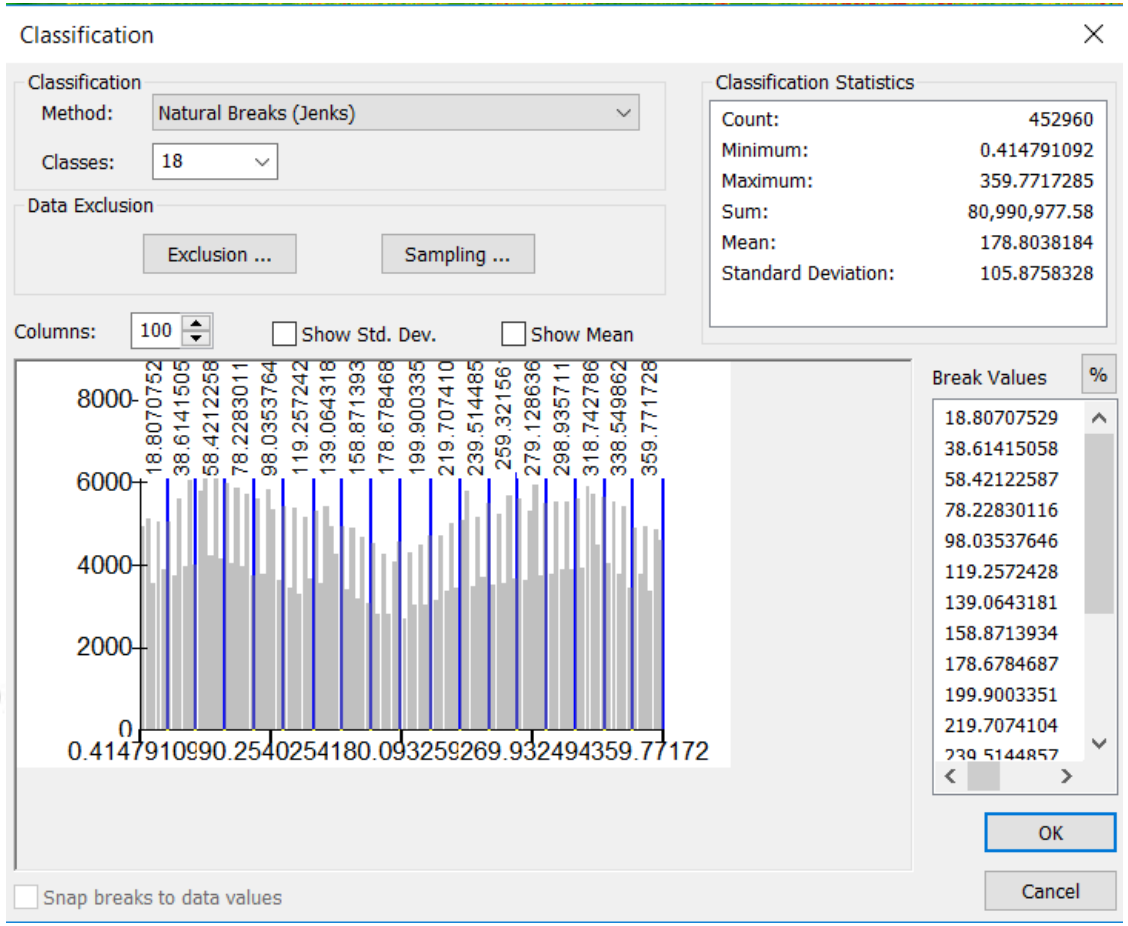

SLOPE GRADIENT STATISTICS

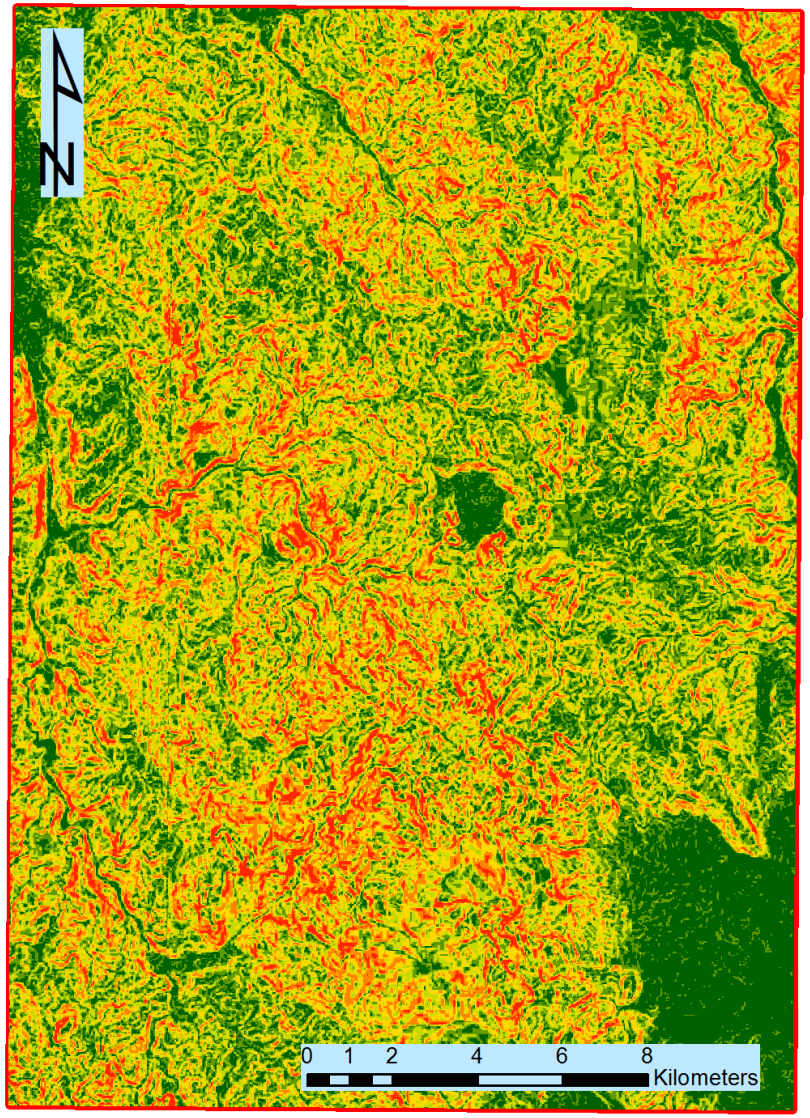

Legend

- 0° - 9 °
- 9° - 15 °
- 15° - 22°
- 22° - 28°
- 28° - 36°
- 36° - 71°

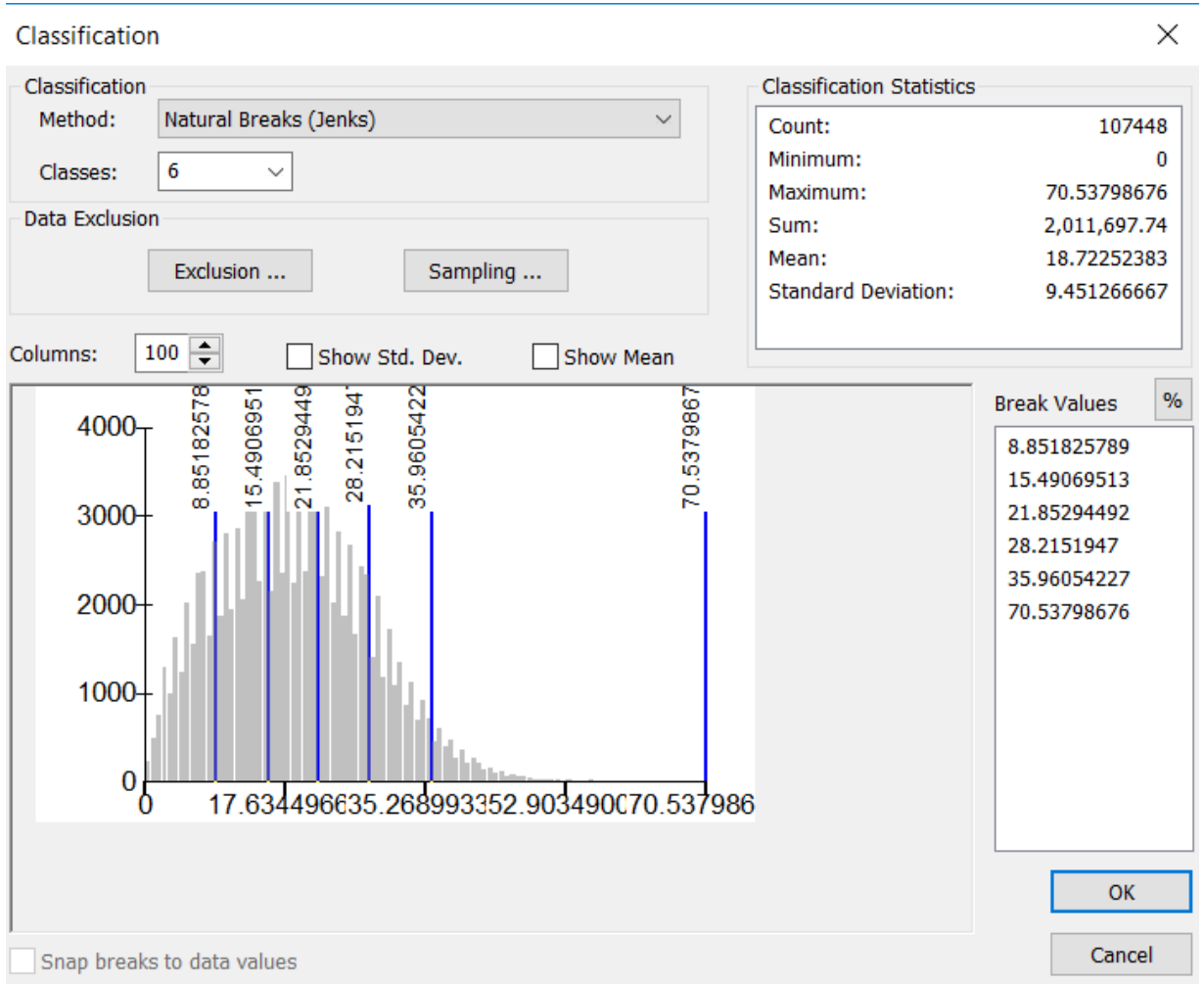

THERMAL MAPPING AND HYDROTHERMAL ALTERATION MAPPING

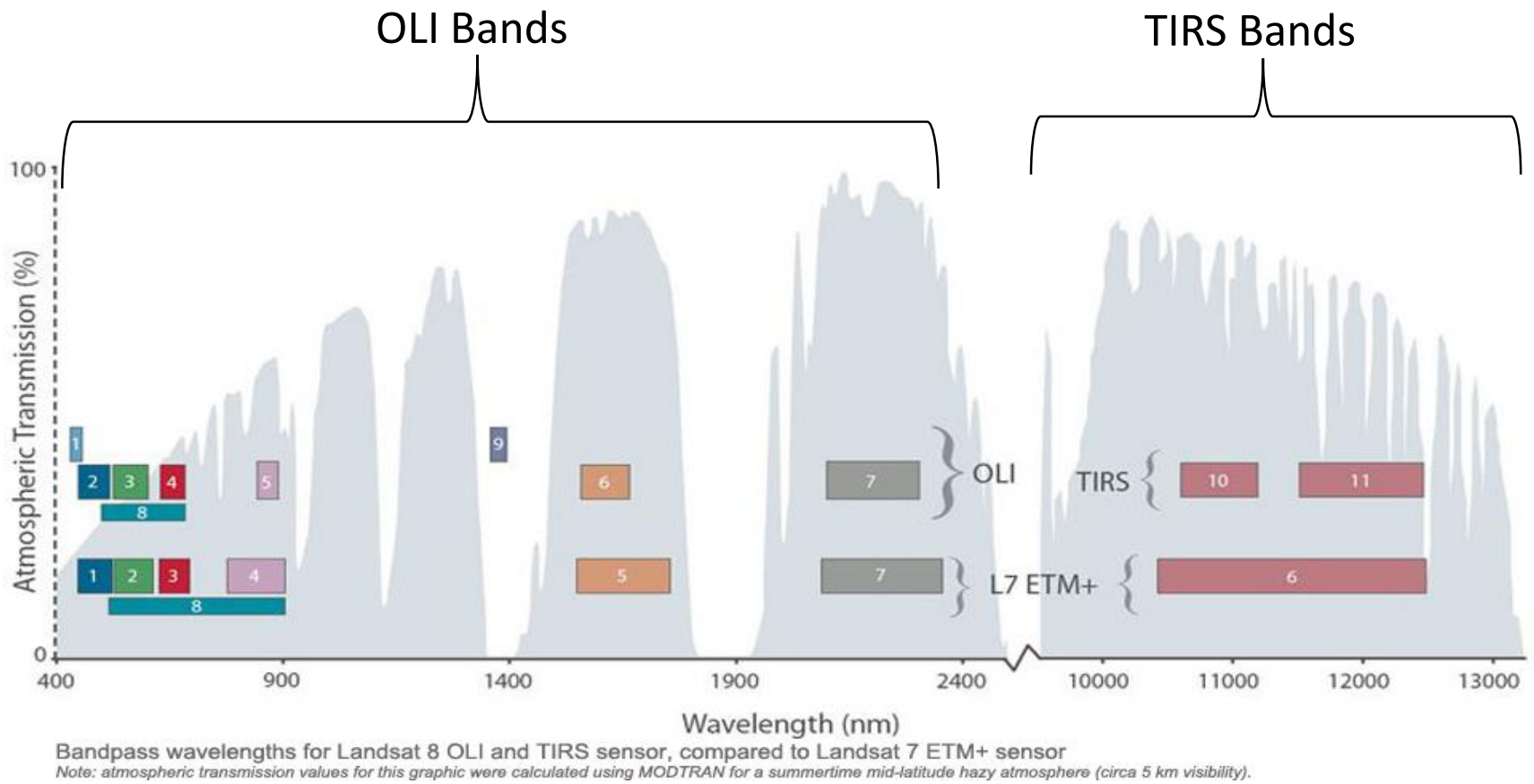

Bandpass wavelengths for Landsat 8 OLI and TIRS sensor, compared to Landsat 7 ETM+ sensor

Note: atmospheric transmission values for this graphic were calculated using MODTRAN for a summertime mid-latitude hazy atmosphere (circa 5 km visibility).

https://landsat.gsfc.nasa.gov/landsat-data-continuity-mission/

THERMAL MAPPING

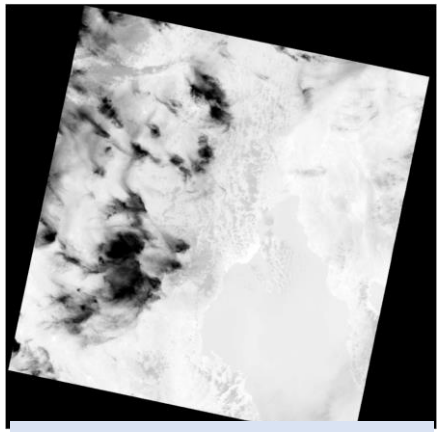

Top of Atmosphere Radiance

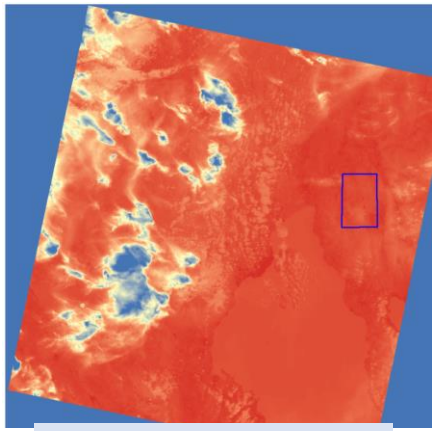

Brightness Temperature

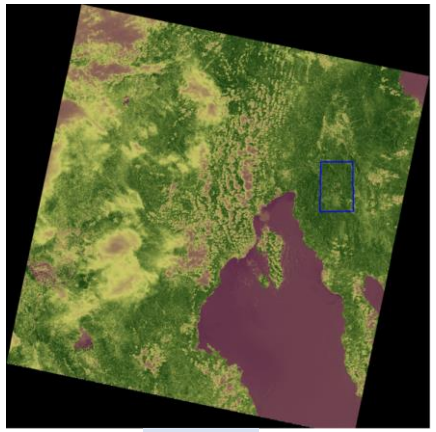

NVDI

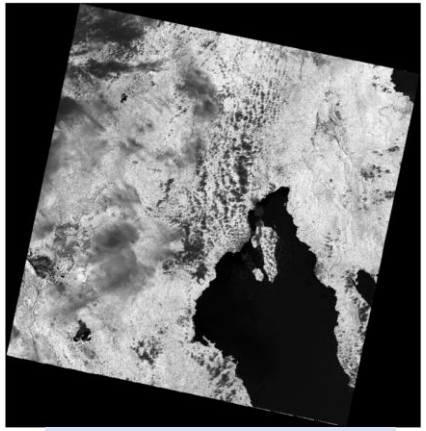

Land Surface Emissivity

$$LST = \frac{BT}{1 + w\left[\left(\frac{BT}{p}\right)(\ln(LSE)]\right]}$$

Where:
LST = Land Surface Temperature
BT = Brightness Temperature
LSE = Land Surface Emissivity
w = wavelength of emitted radiance (11.5 µm in TIRS bands)
p = h x c/s

where: h = Planck's constant (6.626 x 10^{-34} Js)
c = Boltzmann constant (1.38 x 10^{-23} J/K)
s = speed of light (2.998 x 10^{-8} m/s)

LAND SURFACE TEMPERATURE

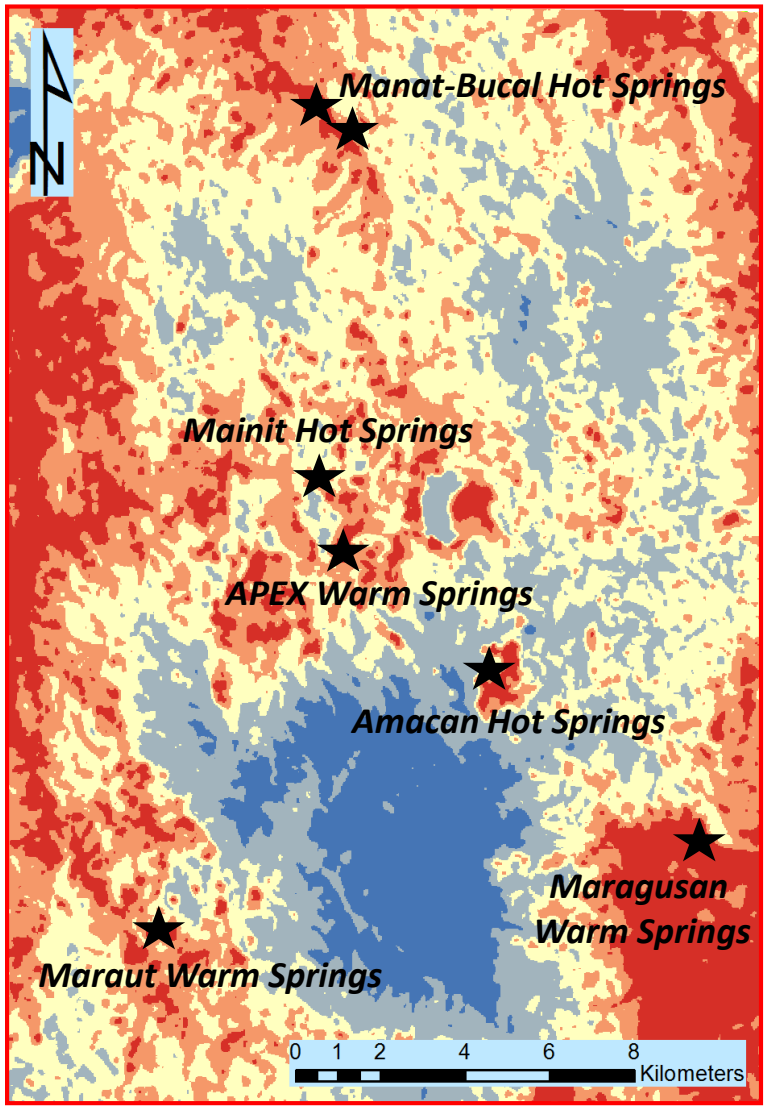

Legend

- 15 - 21°C
- 21 - 23°C
- 23 - 24°C
- 24 - 25°C
- 25 - 31°C

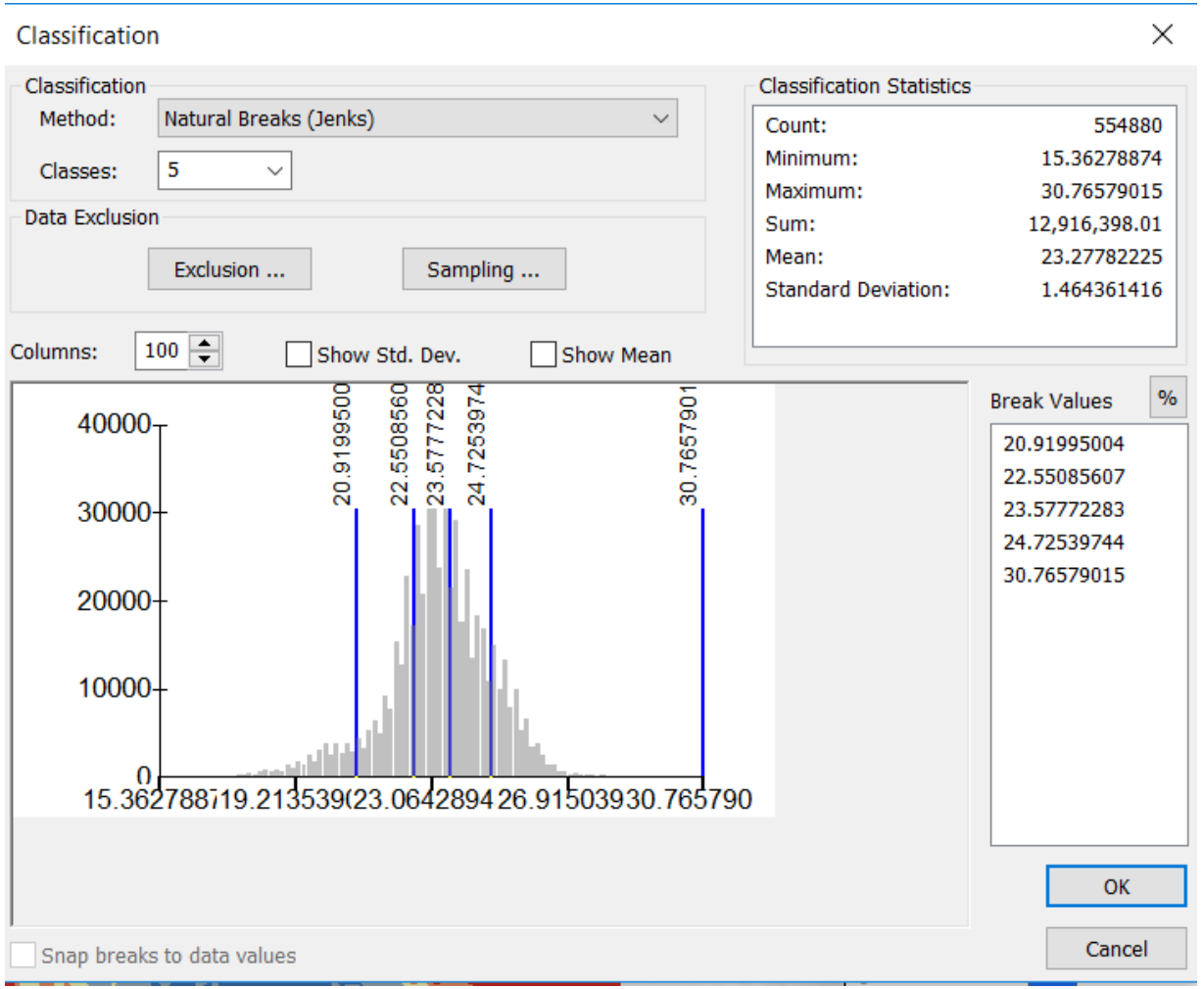

ALTERATION MAPPING

Composite Ratio: RGB = 5:7:6

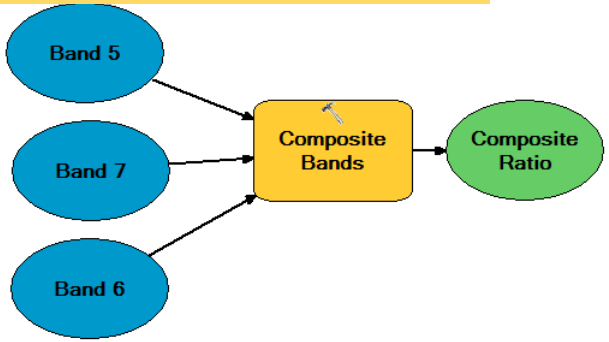

Band Ratio: RGB = 6/7:4/3:5/6

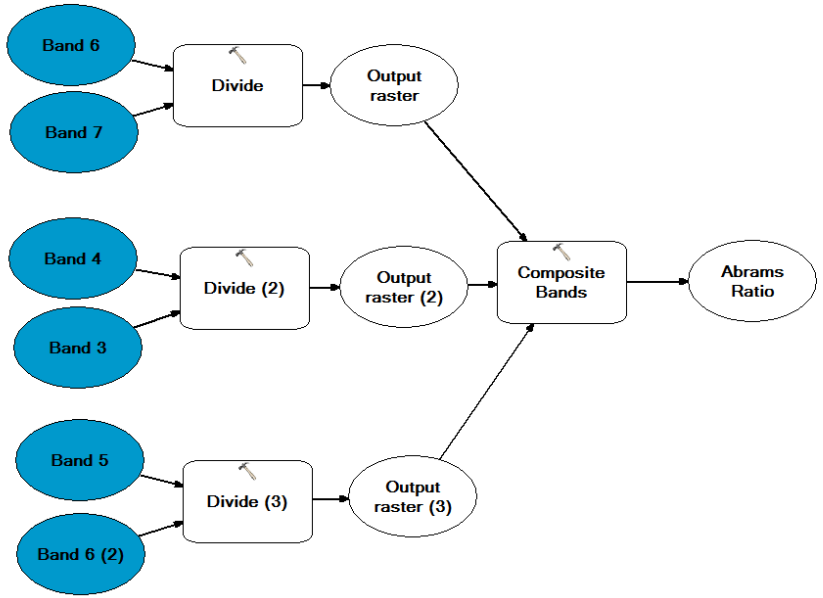

Composite Ratio

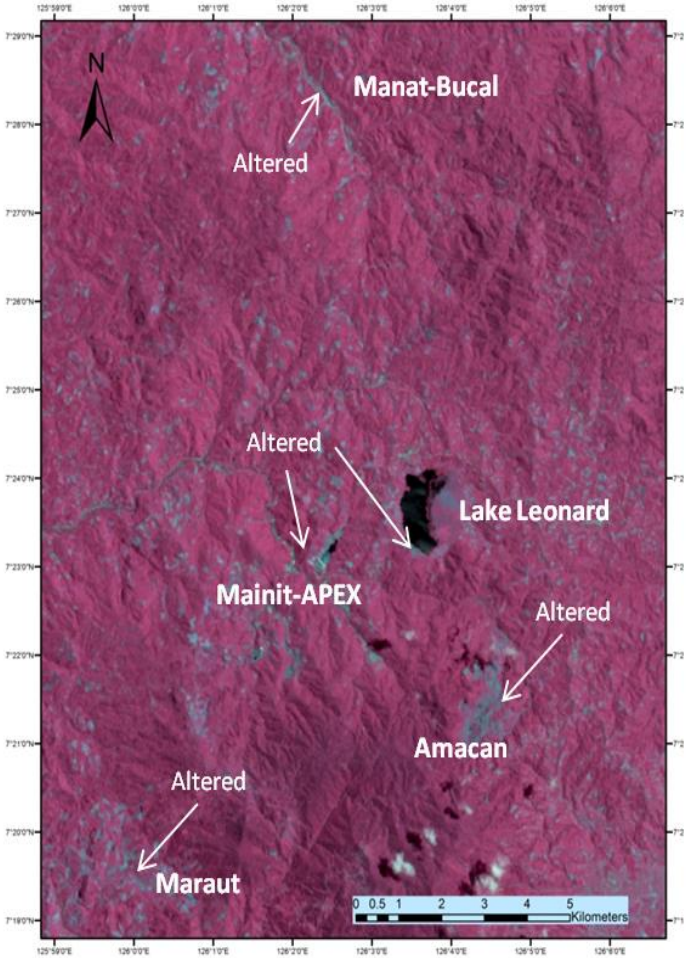

Band Ratio

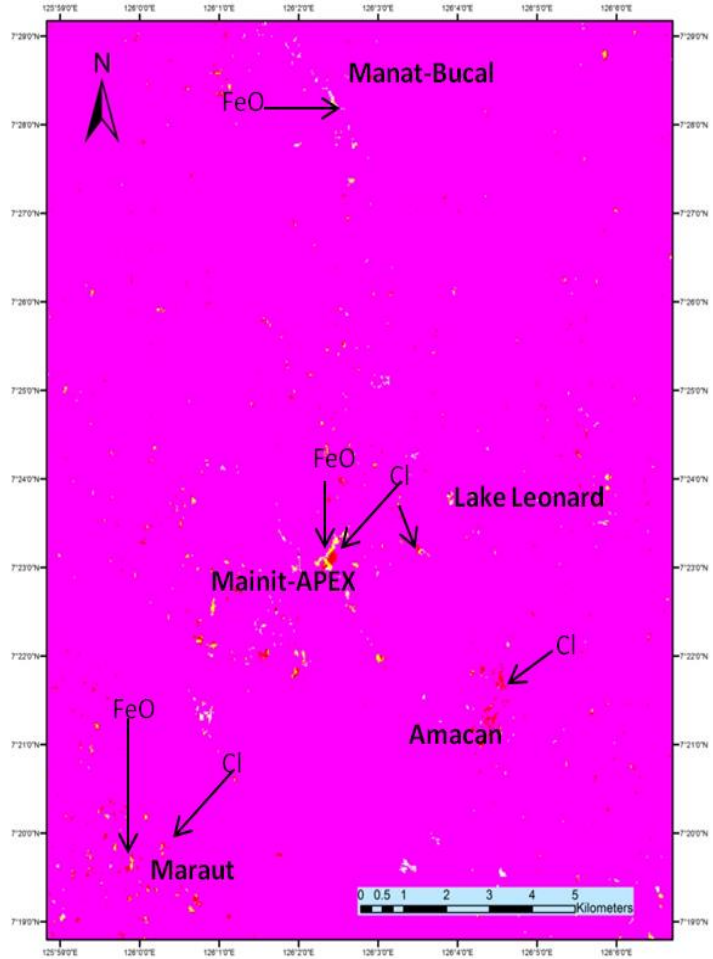

FeO – Iron oxide
Cl - Clay

INTEGRATION

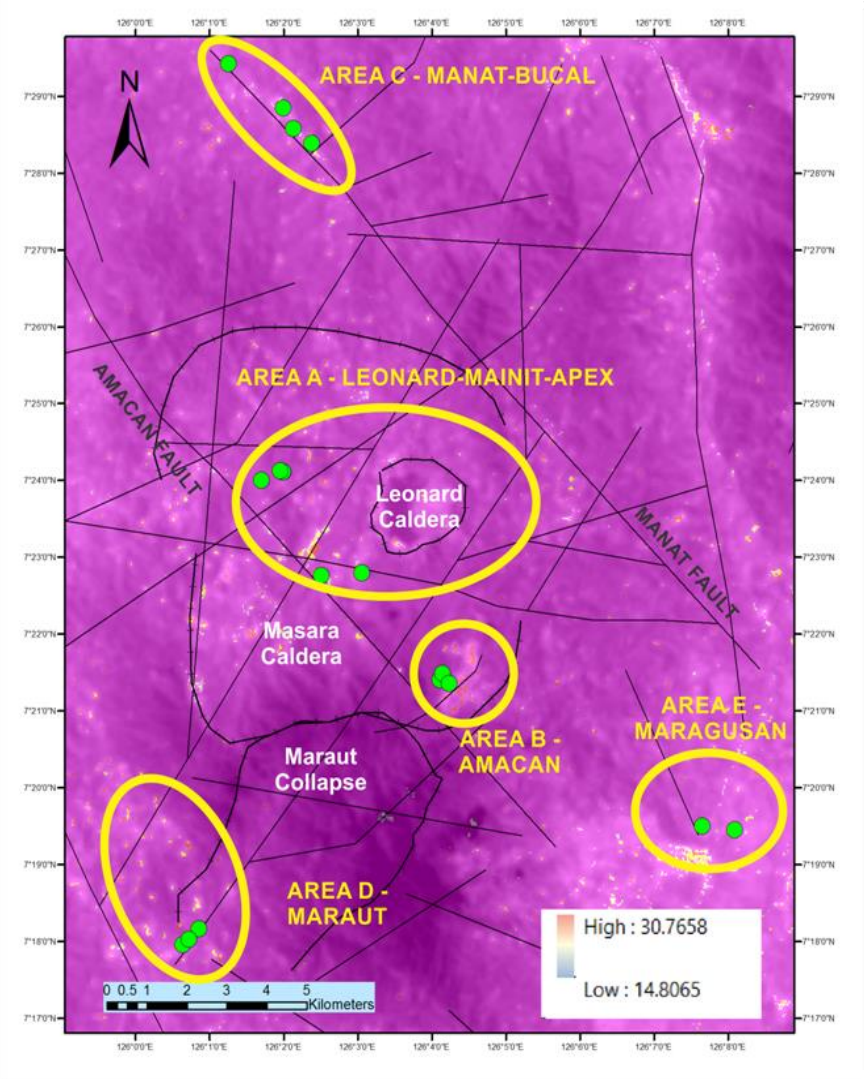

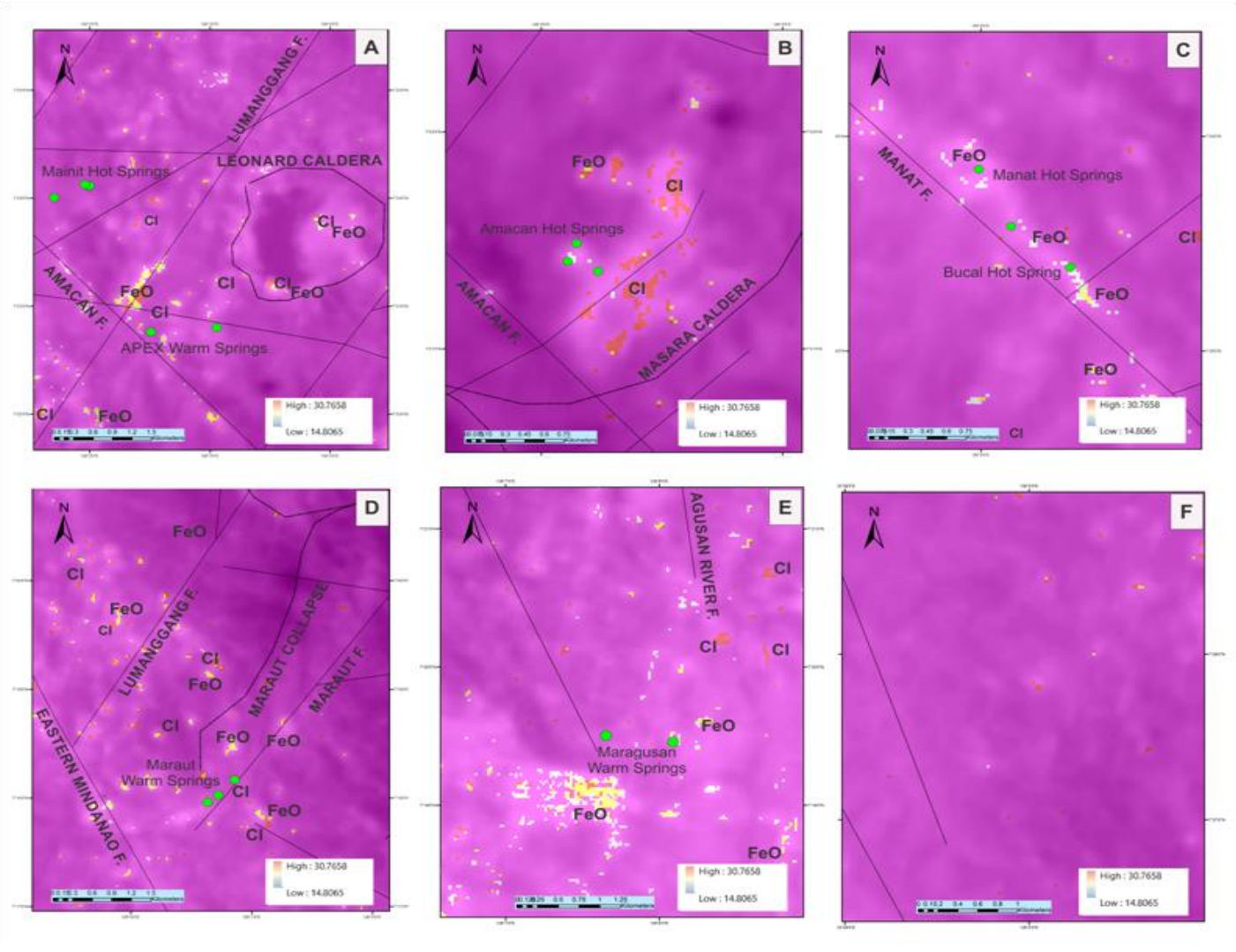

CONCLUSIONS AND RECOMMENDATIONS

- Remote sensing was able to use freely available data to gain preliminary information on the Amacan Geothermal Prospect
- As the generated images have large data, statistics was able to give initial impressions on the topography and temperatures. Landsat data was also processed to produce alteration maps.
- Integrating all the results, five priority areas are subject for more detailed geoscientific assessments: Leonard-Mainit-APEX, Amacan, Manat-Bucal, Maraut, and Maragusan

REFERENCES

- Avdan U. and Jovanovska G. (2016) Algorithm for Automated Mapping of Land Surface Temperature Using LANDSAT 8 Satellite Data; *Journal of Sensors*, Volume 2016
- Buhari, U. (2015). Landsat 8: Estimating Land Surface Temperature Using ArcGIS. Retrieved September 22, 2017, from https://www.youtube.com/watch?v=uDQo2a5e7dM
- Buckley, A. (2010). Understanding curvature rasters / ArcGIS Blog., 2017, Retrieved from http://blogs.esri.com/esri/arcgis/2010/10/27/understanding-curvature-rasters
- Braganza, J. (2014). Volcano-tectonic evolution of the Bacon-Manito Geothermal Project, Sorsogon, Philippines (MSc Thesis) The University of Auckland
- Crosta, A. and Moore J. (1989) Enhancement of Landsat Thematic Mapper imagery for residual soil mapping in SW Minais Gerais State, Brazil: A prospecting case history in Greenstone belt terrain; *International Proceedings of the Seventh Thematic Conference: Remote Sensing for Exploration Geology*, pp. 1173–1187
- Hawkins, J.W., Moore, G.F., Villamor, R., Evans, C., and Wright E., 1985, Geology of the composite terranes of east and central Mindanao: *Am. Assoc. Petrol. Geol. Circum-Pacific Council for Energy and Mineral Resources*, Earth Sci. Series, No. 1, p. 437-463.
- Hunt G. R. (1979) Near Infrared (1.3–2.4 μm) spectra of alteration minerals – potential for use in remote sensing; *Geophysics* 44 1974–1986.
- Jensen J. R. (1996) Introductory digital image processing: A remote sensing perspective; 2nd edition, Prentice Hall Series in Geographic Information Science; 318p.
- Mia, B., & Fujimitsu, Y. (2012). Mapping hydrothermal altered mineral deposits using Landsat 7 ETM+ image in and around Kuju volcano, Kyushu, Japan. *Journal Earth System Science* , 1049-1057.
- Poormirzaee R. and Oskouei M.M. (2009) Detection minerals by advanced spectral analysis in ETM+ imagery; *Proceeding of 7th Iranian Student Conference Mining Engineering*, Tabriz, pp. 111–119.
- PHIVOLCS(2002). Leonard . 2018, Retrieved from http://www.phivolcs.dost.gov.ph/html/update_VMEPD/Volcano/VolcanoList/leonardkniaseff.htm
- PHIVOLCS (2015). Distribution of active faults and trenches in the Philippines
- Taranik D. L., Kruse F. A., Goetz A. F. H. and Atkinson W.W. (1991) Remote sensing of ferric iron minerals as guides for gold exploration; *Proceedings Eighth Thematic Conference on Geologic Remote Sensing*, Denver, Colorado, pp. 197–228.
- US Geological Survey (2016). Landsat 8 Data Users Handbook